Biosensors and Bioelectronics 119 (2018) 170–175

Contents lists available at ScienceDirect

Biosensors and Bioelectronics

journal homepage: www.elsevier.com/locate/bios

An enzyme-free electrochemical biosensor combining target recycling with Fe_3O_4/CeO_2@Au nanocatalysts for microRNA-21 detection

Sihan Liu, Zhehan Yang, Yuanyuan Chang, Yaqin Chai*, Ruo Yuan*

Key Laboratory of Luminescent and Real-Time Analytical Chemistry (Southwest University), Ministry of Education, School of Chemistry and Chemical Engineering, Southwest University, Chongqing 400715, PR China

ARTICLE INFO

Keywords:
MicroRNA-21
Nanocatalysts
Catalytic hairpin assembly (CHA)

ABSTRACT

In this study, an electrochemical biosensor was proposed for microRNA-21 detection based on Fe_3O_4/CeO_2 @Au magnetite nanoparticles (Fe_3O_4/CeO_2 @Au MNPs) as nanocatalyst and catalytic hairpin assembly (CHA) for signal application. Firstly, target microRNA-21 hybridized with hairpin H_2 to form H_2-T duplex stranded DNA (dsDNA), which could further open the hairpin H_1 for the formation of H_1-H_2 dsDNA. Simultaneously, the Fe_3O_4/CeO_2 @Au-S_1 not only hybridized with single stranded fragment of H_1-H_2 dsDNA with producing long dsDNA to absorb a large amount of electroactive substances of methylene blue (MB), but also acted as nanocatalyst to directly catalyze the reduction of MB for amplifying the electrochemical signal. Herein, compared with pure Fe_3O_4 nanoparticles, Fe_3O_4/CeO_2 @Au MNPs exhibited excellent catalytic performance since the cerium oxide (CeO_2) nanoparticles and Au nanoparticles can greatly improve the catalytic activity of Fe_3O_4 nanoparticles and effectively prevent the agglomeration of Fe_3O_4 nanoparticles. Owing to the signal amplification strategy, the proposed biosensor provided a wide linear range of 1 fM to 1 nM with a low detection limit of 0.33 fM (defined as S/N = 3) for microRNA-21 detection, and exhibited excellent specificity and sensitivity. This strategy provided a novel avenue for the detection of other biomarkers in electrochemical biosensors.

1. Introduction

MicroRNAs, the small and endogenous non-coding RNAs which regulate over 30% of human genome, are extensively involved in almost every cellular process and significantly related to many human diseases, including cancers, cardiovascular diseases and other neurological disorders (Tian et al., 2018). Since microRNAs were considered of useful diagnostic and prognostic markers, many efforts were employed in microRNAs detection (Catuogno et al., 2011). Conventional detection methods such as northern blotting (Mahdiannasser and Karami, 2018), high-throughput microarrays (Sun et al., 2018) and quantitative polymerase chain reaction (qPCR) (Benes and Castoldi, 2010) suffers from some drawbacks in practical application. For instance, northern blotting has relatively low sensitivity, labor-intensive steps, time-consuming operations and the requirement of a great deal of RNA samples, limiting its broad applications. Although microarray technology can satisfy the need of high throughputs assay, it requires expensive and precise instrument and has poor specificity (Linsen et al., 2009). And the real-time PCR is laborious, easy to occur false positive and requiring highly purified short primer in amplification. In addition, some single molecule detection methods have also been developed. For example, Neely et al. developed a single-molecule method for detecting and quantitating microRNA in biological samples with great sensitivity and specificity (Neely et al., 2005). Zhang et al. developed a single-microbead-based sensing (SMBS) platform, which simply enables the detection of microRNA at the single-molecule level by using microRNA as a model target (Zhang et al., 2015). However, these methods require expensive instruments and the target usually needs preparative enrichment, which are difficult to apply.

Recently, electrochemical biosensors have been widely applied in target analytes for the inherent advantages of simplicity, fast response and low power requirement, which provided a promising method for microRNA detection and disease diagnosis (Kilic et al., 2018). However, the sensitivity of traditional electrochemical methods was unsatisfied, which limited the application of electrochemical biosensors in targets detection. For improving the sensitivity of electrochemical biosensors, many signal amplification approaches were employed such as strand displacement amplification (SDA) (Chen et al., 2018), loop-mediated isothermal amplification (LAMP) (Qi et al., 2018) and rolling circle amplification (RCA) (Zhang et al., 2018a, 2018b, 2018c). For example, Wang et al. described an electrochemical biosensor based on T7 exonuclease assisted cyclic enzymatic amplification for microRNA

* Corresponding authors.
E-mail addresses: yqchai@swu.edu.cn (Y. Chai), yuanruo@swu.edu.cn (R. Yuan).

https://doi.org/10.1016/j.bios.2018.08.006
Received 25 May 2018; Received in revised form 27 July 2018; Accepted 6 August 2018
Available online 08 August 2018
0956-5663/

detection (Wang et al., 2014). Moreover, Dong et al. designed an aptamer strategy based on cyclic enzymatic amplification and aptamer recognition-induced multi-DNA release for exosome detection (Dong et al., 2018). However, these methods are highly dependent on the protein enzyme, which has inherent disadvantages such as the temperature and pH sensitivity, storage difficulties and reactiontime-dependent enzyme activity. Recently, catalytic hairpin assembly (CHA), one of the most promising strategy by target DNA opening a DNA hairpin and then releasing by another DNA hairpins to achieve the target recycling for signal amplification (Zhang et al., 2018a, 2018b, 2018c; Zhao and Ma, 2018), have attracted wide attention. As an enzyme-free amplification strategy, CHA can not only reduce the costs and simplify the detection conditions, but also exhibited a negligible background, indicating a good way for the development of enzyme-free isothermal amplification strategies.

Nanomaterials as nanocatalysts-assisted signal amplification strategies have attracted increasing attention in biomarkers detection to serve as a substitute for some natural enzymes. It has excellent catalytic efficiency and can overcome some disadvantages of natural enzymes, such as the temperature and pH sensitivity, storage difficulties and easy-lose activity. The current research primarily focuses on inorganic nanomaterials, including carbon-based materials (Song et al., 2010; Yin et al., 2009), noble metals (He et al., 2011; Jv et al., 2010), metal oxides (André et al., 2011; Asati et al., 2009), metal organic frameworks (Zhang et al., 2014) and metal sulfides (Dutta et al., 2012; He et al., 2012), which have shown peroxidase-like, oxidase-like, catalase-like, or SOD-like properties. For instance, zheng et al. have reported that Fe_3O_4 nanoparticles can directly catalyze the reduction of small dye molecules such as thionine and methylene blue (Zheng et al., 2014). Fe_3O_4 nanoparticles with good stability and reusability, large specific surface and high surface reactivity have been widely exploited. However, the catalytic activity of Fe_3O_4 nanoparticles is unsatisfied and it is easily oxidized in the air and agglomerated during storage, limiting the application of Fe_3O_4 nanoparticles. Recently, Lin et al. synthesized Fe_3O_4 @MoS_2 composites which exhibit a much better catalyst for the reduction of 4-NP than either MoS_2 or Fe_3O_4 (Lin et al., 2015). The composite materials may not only play the advantage of each component materials, but also bring in unique properties that stem from the synergistic effects of each component materials. It was reported that the cerium oxide (CeO_2) nanoparticles could improve the catalytic activity of Fe_3O_4 nanoparticles (Xu and Wang, 2012), and this new composite material was a competitive candidate of the new catalyst. Inspired by these properties, in this work, Fe_3O_4/CeO_2 MNPs was prepared as catalysts and Au nanoparticles were decorated onto the prepared Fe_3O_4/CeO_2 MNPs to improve the catalytic activity of Fe_3O_4/CeO_2 MNPs and effectively prevent the agglomeration of Fe_3O_4/CeO_2 MNPs.

In this study, we presented a sensitive biosensor based on CHA-induced target recycling and Fe_3O_4/CeO_2 @Au MNPs for microRNA detection (Scheme 1). Firstly, target microRNA-21 hybridized with hairpin H_2 to form H_2-T dsDNA, which could further open the H_1 hairpin structure for the formation of H_1-H_2 dsDNA on the electrode. Meanwhile, the target was released to participate in the next cycle to produce plenty of H_1-H_2 dsDNA for signal amplification. And then the part of newly emerged H_1-H_2 dsDNA could bound with single DNA S_1 which labeled the Fe_3O_4/CeO_2 @Au (Fe_3O_4/CeO_2 @Au-S_1). With the catalysis of Fe_3O_4/CeO_2 @Au MNPs to MB intercalated into dsDNA, a strong current signal could be obtained. Compared with Fe_3O_4 nanoparticles, Fe_3O_4/CeO_2 @Au MNPs exhibited excellent catalytic performance since the cerium oxide (CeO_2) nanoparticles and Au nanoparticles can greatly improve the catalytic activity of Fe_3O_4 nanoparticles and effectively prevent the agglomeration of Fe_3O_4 nanoparticles. In all, based on the enzyme-free target recycling and Fe_3O_4/CeO_2 @Au MNPs for signal amplification, the electrochemical biosensor exhibited rapid and sensitive detection of microRNA-21.

2. Experimental

2.1. Preparation of Fe_3O_4/CeO_2 @Au- S_1

The Fe_3O_4/CeO_2 @Au MNPs was synthesized according to the literature (Gan et al., 2017) with slight modifications. Firstly, 0.5460 g $FeC1_3{\cdot}6H_2O$, 0.1988 g $FeC1_2{\cdot}4H_2O$ and 0.4340 g $Ce(NO_3)_3{\cdot}6H_2O$ were dissolved in 50 mL double-distilled water under vigorous magnetic stirring at room temperature. Then, 0.1 mL hydrochloric acid (1 M) was added to stir 5 min under ambient temperature. Afterwards, 25 mL ammonia (25 wt%) was dropped into a four-necked flask containing the previous solution with vigorous stirring under N_2 protecting at 65 °C for 15 min. The resulted solution was maintained at 160 °C for 5 h in a Teflon-lined stainless-steel autoclave. After centrifuging and washing with ethanol and water respectively, the nanoparticles were dried in a vacuum drying oven for instant usage to obtain the Fe_3O_4/CeO_2 MNPs. Subsequently, the bovine serum albumin (BSA) was used to modify the surface of the Fe_3O_4/CeO_2 MNPs to obtain the amido and disulfides groups modified Fe_3O_4/CeO_2 MNPs. Then 100 mL AuNPs which synthesized according to the literature (Chen et al., 2015) was added to the resultant Fe_3O_4/CeO_2 MNPs and stirred for 10 h to obtain the Fe_3O_4/CeO_2 @Au MNPs. Finally, 200 μL S_1 (2 μM) was mixed and stirred with 1 mL of the above Fe_3O_4/CeO_2 @Au MNPs overnight at 4 °C for the formation of Fe_3O_4/CeO_2 @Au-S_1, which was then centrifuged and washed for three times with water and then resuspended in Tris-HCl buffer. All the products were stored at 4 °C for further use.

2.2. Preparation of the functionalized electrode

The glassy carbon electrode (GCE) (Φ = 4 mm) was polished with 0.3 μm alumina slurry for obtaining a mirror-like surface, and then the GCE were washed with water-ethanol-water in turn and dried in room temperature. Later, the GCE was electrodeposited in $HAuCl_4$ solution for 30 s to obtain a layer of bright Au nanoparticle (AuNPs), and then incubated with 10 μL H_1 (2 mM) overnight. Finally, the modified GCE was blocked with 10 μL HT (1 mM) for 40 min.

2.3. The measurement procedure

With the help of different concentration of target microRNA, 20 μL H_2 (2 μM) was incubated at the modified GCE for 2 h at room temperature to obtain plenty of H_1-H_2 dsDNA. After rinsing with double-distilled water, 10 μL Fe_3O_4/CeO_2 @Au-S_1 was incubated on the GCE for 2 h to hybridize with single stranded fragment of H_1-H_2 dsDNA for obtaining a long dsDNA (H_1-H_2-S_1). Finally, 10 μL MB (1 mM) was incubated on the GCE for 2 h, which was intercalated into dsDNA (H_1-H_2-S_1) and serve as electroactive substances. The more target microRNA was input, the more dsDNA (H_1-H_2-S_1) which contained MB was generated. Thus, the biosensor could be used for target microRNA detection.

3. Results and discussion

3.1. Characterizations of the prepared nanoparticles

The prepared nanoparticles of Fe_3O_4/CeO_2 MNPs and Fe_3O_4/CeO_2 @Au MNPs were characterized by transmission electron microscope (TEM) and X-ray photoelectron spectroscopy (XPS) (Fig S2). Fig. 1A showed the TEM image of Fe_3O_4/CeO_2 MNPs. The Fe_3O_4/CeO_2 MNPs displayed sphere structure and good dispersion with the diameter of about 20 nm. And Fig. 1B showed the TEM image of Fe_3O_4/CeO_2 @Au MNPs. It could be observed that the AuNPs were adsorbed on the surface of the Fe_3O_4/CeO_2 MNPs, illustrating the successful decorated of Fe_3O_4/CeO_2 @Au MNPs.

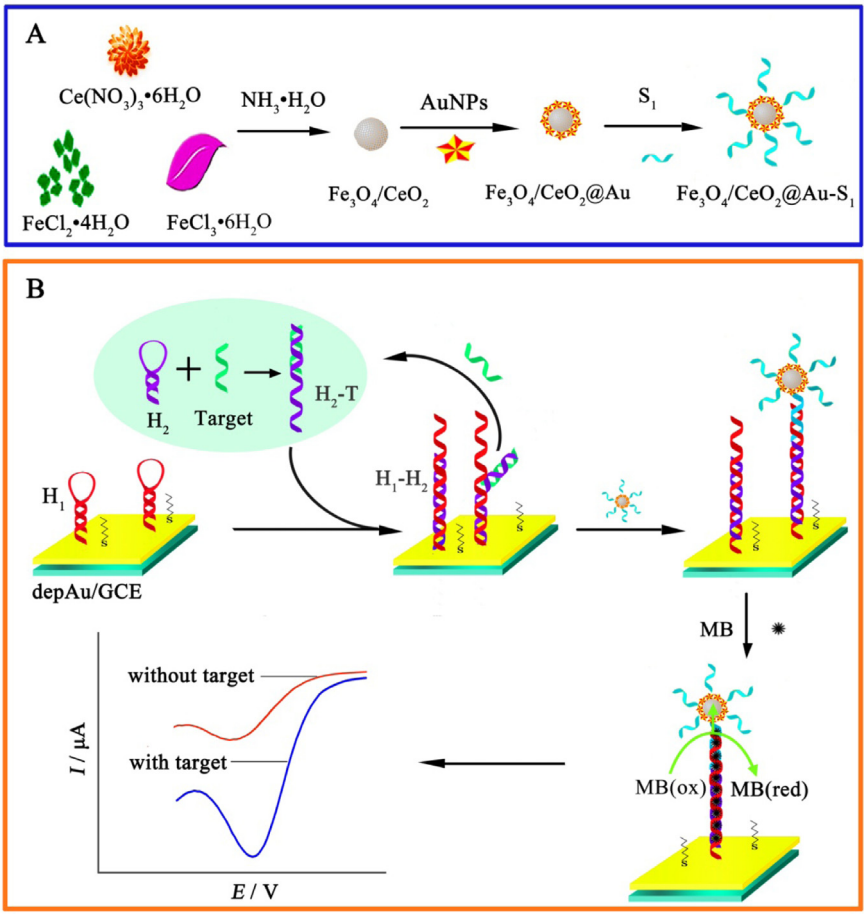

Scheme 1. Schematic diagram of the fabrication process of a biosensor: (A) preparation procedure of Fe_3O_4/CeO_2 @Au-S_1, (B) signal amplification strategy and the detection principle for microRNA-21.

3.2. Electrochemical characterization of the proposed biosensor

Fig. 2A shows the EIS of the fabrication process of the biosensor in 5 mM $[Fe(CN)_6]^{3-/4-}$ (containing 0.1 M KCl, pH = 7.0). The bare GCE revealed a small semicircle diameter (curve a). Then, the semicircle diameter was decreased significantly with AuNPs electrodepositing on the GCE (curve b). The semicircle diameter increased obviously (curve c) as H_1 immobilizing on the GCE, because H_1 acted as a nonconductor to block the electron transfer. Subsequently, the HT was dripped onto the GCE to block the unreaction sites, leading to a increased semicircle diameter (curve d). As expected, the semicircle diameter was further increased when the mixture of H_2 and target (10 pM) was incubated on the modified GCE (curve e). All these results were in good agreement with the rationale, which proved the successful assemble process of the biosensor.

3.3. Electrochemical comparison of various labeled probes

To demonstrate the feasibility of the proposed nanocatalysts amplification strategy, the electrode modified with various labeled probes was investigated by DPV measurement in 2 mL PBS solution (0.1 M, pH = 7). The parameters applied were: potential range from −0.36 to −0.1 V, 50 mV modulation amplitude, 20 ms pulse width, and 0.5 s pulse period. As shown in Fig. 2B, when the biosensor was incubated with PBS buffer, a low current response (curve a) could be observed. Once the Fe_3O_4 @Au-S_1 was incubated on the GCE surface, an increased

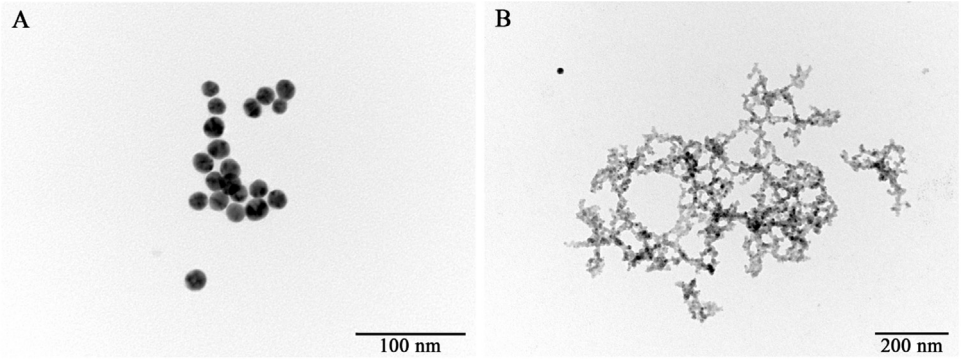

Fig. 1. TEM images of (A) Fe_3O_4/CeO_2 MNPs, (B) Fe_3O_4/CeO_2 @Au MNPs.

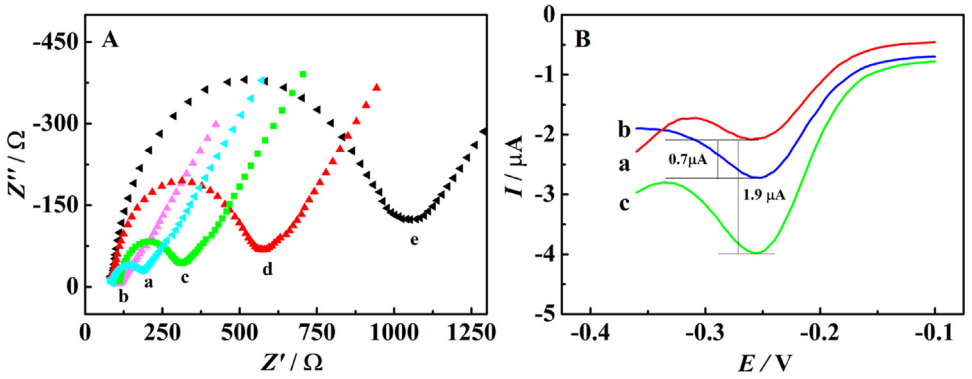

Fig. 2. (A)The fabrication process of the biosensor: EIS of (a) bare GCE, (b) AuNPs/GCE, (c) H_1/AuNPs/GCE, (d) HT/H_1/AuNPs/GCE, (e) H_2/Target/HT/H_1/AuNPs/GCE. (B) DPV curves of the biosensor under different conditions (a) with PBS buffer, (b) with Fe_3O_4 @Au-S_1, (c) with Fe_3O_4/CeO_2 @Au-S_1.

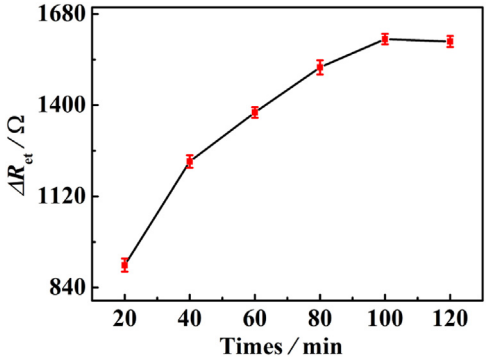

Fig. 3. The optimization of CHA reaction time by EIS response.

current response could be observed, suggesting the electrocatalytic activities of Fe_3O_4 nanoparticles toward the electrochemical reduction of MB (curve b). Upon addition of Fe_3O_4/CeO_2 @Au-S_1, a significant increased of the current response could be observed (curve c), indicating that the Fe_3O_4/CeO_2 @Au-S_1 possessed better electrocatalytic activities than Fe_3O_4 @Au-S_1.

3.4. Optimum of CHA reaction time

In order to maximize the performance of the proposed biosensor, the relationship between the reaction time of CHA and the response of EIS was also evaluated. It can be seen from the Fig. 3, as the reaction time of CHA shifted from 20 to 120 min, the electrochemical response increased and reached the maximum at 100 min, indicating the saturation of the hybridization reaction. Therefore, 100 min was selected as the reaction time.

3.5. Analytical performance of the electrochemical biosensor

The analytical performance of the biosensor was invested by the detection of microRNA-21 under the optimized conditions. As shown in Fig. 4A, with the concentrations of microRNA-21 increasing from 1 fM to 1 nM, the current signal of biosensor increased accordingly. And as shown in Fig. 4B, the current signal performed a linear relationship with the logarithms of target microRNA-21 with a detection limit of 0.33 fM. The regression equation was I= -1.977 lg c-3.796 (r = 0.9961, I is the current signal and c is the concentrations of microRNA-21). Table 1 compared our microRNA biosensor with other reported microRNA detection methods. As shown, the analytical performance of the developed biosensor exhibited well.

3.6. Specificity, reproducibility and stability of the proposed biosensor

Furthermore, specificity, reproducibility and stability were key factors which fully reflected the value of the biosensor. To evaluate the specificity of the biosensor, some related interferences including blank (PBS buffer), microRNA-141, microRNA-155 and microRNA-199 were employed to the DPV study, and the results were exhibited in Fig. 5. The high DPV response could be observed after the biosensor was incubated with target microRNA-21 or the mixture containing the target microRNA-21. When the other microRNAs were employed to DPV detection, the responses were close to the blank reagents, indicating the high selectivity of our biosensor.

The reproducibility of the biosensor had been evaluated by incubating the same microRNA-21 concentration on the four prepared electrodes in the same conditions (Fig. S3). The four electrodes showed similar currents signals with a relative standard deviation (RSD) of 5.8% (n = 4), indicating that the reproducibility of the biosensor was

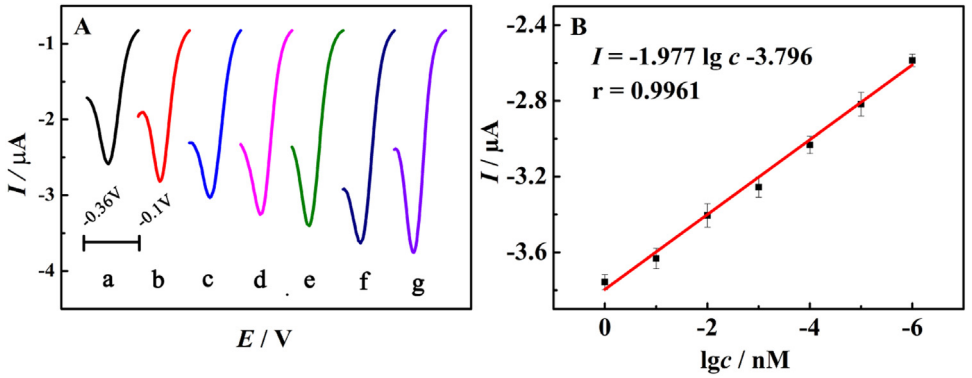

Fig. 4. (A) DPV responses of the proposed biosensor with different microRNA-21 concentrations (a:1 fM, b:10 fM, c:100 fM, d:1 pM, e:10 pM, f:100 pM, g:1 nM). (B) The calibration plots of DPV peak current vs the logarithm of microRNA-21 concentration.

Table 1
Comparison of analytical performance between proposed biosensors and other works for microRNA detection.

methods	detection limit	dynamic range	references
ECL	10 fM	10 fM to 10 pM	(Liao et al., 2014)
ECL	21.7 fM	100 fM to 100 nM	(Cheng et al., 2014)
Fluorescence	300 fM	1 pM to 100 nM	(Xi et al., 2014)
Fluorescence	58 fM	100 fM to 1 nM	(Li et al., 2016)
DPV	1.2 fM	10 fM to 100 nM	(Tian et al., 2015)
DPV	45 fM	100 fM to 10 pM	(Xia et al., 2013)
DPV	67 a.M.	0.1–100 fM	(Zhang et al., 2018a, 2018b, 2018c)
single molecule arrays	500 fM	10 pM to 10 nM	(Rissin et al., 2017)
photoluminescence	1–60 miRNA copies	10 fM to 100 pM	(Harvey et al., 2017)
DPV	0.33 fM	1 fM to 1 nM	This work

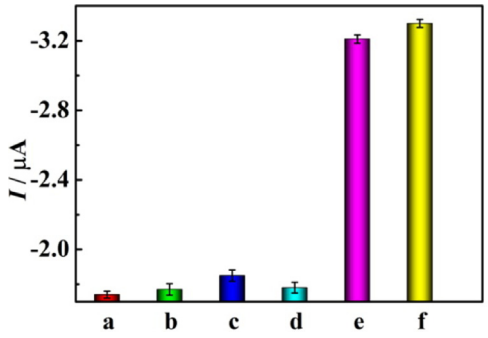

Fig. 5. Specificity of the biosensor detection of different microRNA (a: blank (PBS buffer) b: microRNA-141 (1 nM), c: microRNA-155 (1 nM), d: microRNA-199 (1 nM), e: microRNA-21 (0.1 nM), f: the mixture of microRNA-21 (0.1 nM), microRNA-141 (1 nM), microRNA-155 (1 nM) and microRNA-199 (1 nM)).

Table 2
Determination of microRNA-21 added in human serum with the proposed biosensor.

Serum sample	Add/pM	Found/pM	Recovery/%	RSD/%
1	0.1	0.1062	106.2	4.3
2	1.0	0.9962	99.62	6.2
3	10.0	9.557	95.57	5.5
4	100.0	100.2	100.2	4.6

acceptable.

The long-term storage stability of the proposed biosensor was investigated over a period of 20 days of storage (at 4 °C) (Fig. S4). The signal intensity decreased gradually and retained 90.2% of its initial current after 10 days and 81.6% after 20 days, suggesting that the stability of the biosensor was acceptable.

3.7. Real sample analysis of microRNA-21

The feasibility of the biosensor was investigated by adding microRNA-21 of different concentrations to 10-fold-diluted normal human serum samples. The serum samples were gently shaken for 5 min at room temperature, and then were measured by biosensor developed in this work. As shown in Table 2, the recoveries were ranging from 95.57% to 106.2%, suggesting that the proposed biosensor had potential in detection of microRNA-21 in real samples.

4. Conclusion

In summary, we designed an ultrasensitive electrochemical biosensor based on Fe_3O_4/CeO_2 @Au MNPs as nanocatalyst and CHA for signal application for microRNA-21 detection. Firstly, Fe_3O_4/CeO_2 @Au MNPs exhibited excellent catalytic performance since the cerium oxide (CeO_2) nanoparticles and Au nanoparticles can greatly improve the catalytic activity of Fe_3O_4 nanoparticles and effectively prevent the agglomeration of Fe_3O_4 nanoparticles. Secondly, CHA, the enzyme-free DNA circuits that rely on toehold-mediated DNA strand displacement, was introduced into microRNA-21 detection, which can overcome some disadvantages of protein enzymes to further enhanced signal response. Owing to the signal amplification strategy, the proposed biosensor provided a wide linear range and a low detection limit for microRNA-21 detection, providing a novel avenue for the detection of other biomarkers in electrochemical biosensors.

Acknowledgments

This paper was financially supported by the National Natural Science Foundation of China (21675129, 21775124, 21575116 and 51473136) and the Fundamental Research Funds for the Central Universities (XDJK2018AA003), China.

Appendix A. Supplementary material

Supplementary data associated with this article can be found in the online version at doi:10.1016/j.bios.2018.08.006.

References

André, R., Natálio, F., Humanes, M., Leppin, J., Heinze, K., Wever, R., Schröder, H.C., Müller, W.E.G., Tremel, W., 2011. Adv. Funct. Mater. 21, 501–509.
Asati, A., Santra, S., Kaittanis, C., Nath, S., Perez, J.M., 2009. Angew. Chem. Int. Ed. 48, 2308–2312.
Benes, V., Castoldi, M., 2010. Methods 50, 244–249.
Catuogno, S., Esposito, C.L., Quintavalle, C., Cerchia, L., Condorelli, G., Franciscis, V.D., 2011. Cancers 3, 1877–1898.
Chen, M., Kang, H., Gong, Y., Guo, J., Zhang, H., Liu, R., 2015. Acs. Appl. Mater. Interfaces 7, 21717–21726.
Chen, Y., Huang, K., Niu, K., 2018. Biosens. Bioelectron. 99, 612–624.
Cheng, Y., Lei, J., Chen, Y., Ju, H., 2014. Biosens. Bioelectron. 51, 431–436.
Dong, H., Chen, H., Jiang, J., Zhang, H., Cai, C., Shen, Q., 2018. Anal. Chem. 90, 4507–4513.
Dutta, A.K., Maji, S.K., Srivastava, D.N., Mondal, A., Biswas, P., Paul, P., Adhikary, B., 2012. Acs. Appl. Mater. Interfaces 4, 1919–1927.
Gan, G., Liu, J., Zhu, Z., Yang, Z., Zhang, C., Hou, X., 2017. Chemosphere 168, 254–263.
Harvey, J.D., Jena, P.V., Baker, H.A., Zerze, G.H., Williams, R.M., Galassi, T.V., Roxbury, D., Mittal, J., Heller, D.A., 2017. Nat. Biomed. Eng. 1, 41.
He, W., Jia, H., Li, X., Lei, Y., Li, J., Zhao, H., Mi, L., Zhang, L., Zheng, Z., 2012. Nanoscale 4, 3501–3506.
He, W., Liu, Y., Yuan, J., Yin, J.J., Wu, X., Hu, X., Zhang, K., Liu, J., Chen, C., Ji, Y., 2011. Biomaterials 32, 1139–1147.
Jv, Y., Li, B., Cao, R., 2010. Chem. Commun. 46, 8017–8019.
Kilic, T., Erdem, A., Ozsoz, M., Carrara, S., 2018. Biosens. Bioelectron. 99, 525–546.
Li, L., Feng, J., Liu, H., Li, Q., Tong, L., Tang, B., 2016. Chem. Sci. 7, 1940–1945.
Liao, Y., Huang, R., Ma, Z., Wu, Y., Zhou, X., Xing, D., 2014. Anal. Chem. 86, 4596–4604.
Lin, T., Wang, J., Guo, L., Fu, F., 2015. J. Phys. Chem. C 119, 13658–13664.
Linsen, S.E., De, W.E., Janssens, G., Heater, S., Chapman, L., Parkin, R.K., Fritz, B., Wyman, S.K., De, B.E., Voest, E.E., 2009. Nat. Methods 6, 474.
Mahdiannasser, M., Karami, Z., 2018. Biosens. Bioelectron. 123–144.
Neely, L.A., Patel, S., Garver, J., Gallo, M., Hackett, M., McLaughlin, S., Nadel, M., Harris, J., Gullans, S., Rooke, J., 2005. Nat. Methods 3, 41.
Qi, H., Yue, S., Bi, S., Ding, C., Song, W., 2018. Biosens. Bioelectron. 110, 207–217.
Rissin, D.M., Lópezlongarela, B., Pernagallo, S., Ilyine, H., Adb, V., Dear, J.W., Díazmochón, J.J., Duffy, D.C., 2017. PLoS One 12.
Song, Y., Qu, K., Zhao, C., Ren, J., Qu, X., 2010. Adv. Mater. 22, 2206.

Sun, X., Wang, H., Wang, Y., Gui, T., Wang, K., Gao, C., 2018. Biosens. Bioelectron. 102, 63–69.
Tian, L., Qian, K., Qi, J., Liu, Q., Yao, C., Song, W., Wang, Y., 2018. Biosens. Bioelectron. 99, 564–570.
Tian, Q., Wang, Y., Deng, R., Lin, L., Liu, Y., Li, J., 2015. Nanoscale 7, 987–993.
Wang, M., Fu, Z., Li, B., Zhou, Y., Yin, H., Ai, S., 2014. Anal. Chem. 86, 5606–5610.
Xi, Q., Zhou, D.M., Kan, Y.Y., Ge, J., Wu, Z.K., Yu, R.Q., Jiang, J.H., 2014. Anal. Chem. 86, 1361–1365.
Xia, N., Zhang, L., Wang, G., Feng, Q., Liu, L., 2013. Biosens. Bioelectron. 47, 461–466.
Xu, L., Wang, J., 2012. Environ. Sci. Technol. 46, 10145–10153.
Yin, J.J., Lao, F., Fu, P.P., Wamer, W.G., Zhao, Y., Wang, P.C., Qiu, Y., Sun, B., Xing, G., Dong, J., 2009. Biomaterials 30, 611–621.
Zhang, J., Wang, L., Hou, M., Xia, Y., He, W., Yan, A., Weng, Y., Zeng, L., Chen, J., 2018. Biosens. Bioelectron. 102, 33–40.
Zhang, J.W., Zhang, H.T., Du, Z.Y., Wang, X., Yu, S.H., Jiang, H.L., 2014. Chem. Commun. 50, 1092–1094.
Zhang, K., Lv, S., Lin, Z., Li, M., Tang, D., 2018. Biosens. Bioelectron. 101, 159–166.
Zhang, X., Liu, C., Sun, L., Duan, X., Li, Z., 2015. Chem. Sci. 6, 6213–6218.
Zhang, Y., Luo, S., Situ, B., Chai, Z., Li, B., Liu, J., Zheng, L., 2018. Biosens. Bioelectron. 102, 568–573.
Zhao, J., Ma, Z., 2018. Biosens. Bioelectron. 102, 316–320.
Zheng, T., Zhang, Q., Feng, S., Zhu, J.J., Wang, Q., Wang, H., 2014. J. Am. Chem. Soc. 136, 2288–2291.